NANO LETTERS

Letter

pubs.acs.org/NanoLett

Nanoblade Delivery and Incorporation of Quantum Dot Conjugates into Tubulin Networks in Live Cells

Jianmin Xu,[†] Tara Teslaa,[‡] Ting-Hsiang Wu,[§] Pei-Yu Chiou,[§,#] Michael A. Teitell,[‡,⊥,#] and Shimon Weiss*[,†,∥,#]

[†]Department of Chemistry & Biochemistry, [‡]Department of Pathology and Laboratory Medicine, [§]Department of Electrical Engineering, [∥]Department of Physiology, [⊥]Molecular Biology Institute, [#]California NanoSystems Institute, University of California, Los Angeles, Los Angeles, California 90095, United States

Supporting Information

ABSTRACT: Quantum dots (QDs) have not been used to label cytoskeleton structure of live cells owing to limitations in delivery strategies, and QDs conjugation methods and issues with nonspecific binding. We conjugated tubulin to QDs and applied the emerging method of photothermal nanoblade to deliver QD-tubulin conjugates into live Hela cells. This method will open new opportunities for cytosolic targeting of QDs in live cells.

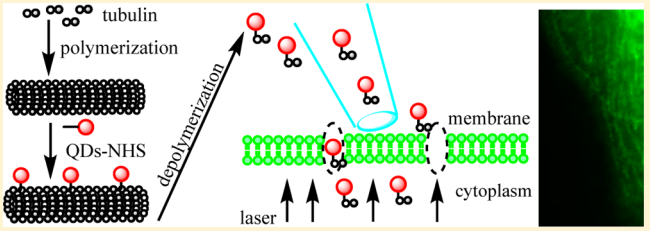

KEYWORDS: *Nanoblade delivery, QD-tubulin, cytosolic targeting*

Since their introduction as biological imaging probes,[1,2] quantum dots (QDs) have gained prominence in various imaging applications due to their unique attributes such as high brightness, broad excitation spectrum, narrow emission spectrum, and excellent photostability.[3−5] However, QDs also suffer from several shortcomings such as relatively large size,[6] nonspecific binding (due to the charge of surface coatings),[7,8] large avidity,[9] blinking,[10,11] and cytotoxicity.[12] These shortcomings have restricted the general utility for quantum dots to only a subset of imaging applications.

An important, but elusive, goal has been the delivery and labeling of QDs to cytosolic targets. Such a capability would enable multiplexed detection and single particle tracking of transiently interacting proteins and dynamic cellular machines over long periods of times. Successful cytosolic targeting requires, however, an efficient delivery that escapes the endocytotic pathway, supplying QDs to the cytosol that is not engulfed in membranous organelles (endosome-free QDs). In addition, once delivered, QDs should have minimal steric hindrance (i.e., small size) and minimal nonspecific binding so that they can freely diffuse and sample the full cytosolic volume in order to find and specifically bind to their target(s).

Although extensive efforts have been vested in developing cytosolic targeting methods and many reports claim to have achieved successful targeting,[13] a general and widely applicable protocol that offers infallible demonstrations of specific cytosolic targeting of fine structures such as the cytoskeleton are still lacking. Conventional methods can be classified into two main categories: (i) Facilitated delivery strategies such as, using cell penetrating peptides (CPP),[14,15] proton sponge polymer carriers,[16,17] pinocytosis,[18,19] and transfection reagents.[18] Methods belonging to this category provide high throughput delivery, but suffer from low efficiency release of endosome-free QDs (i.e., most QDs end up trapped in endosomes). (ii) Active delivery methods include electroporation[20,21] and microinjection.[22] Electroporation offers an efficient way of delivery by temporarily destabilizing the plasma membrane to create transient pores using high voltage electrical pulses. However, this method suffers from low cell viability, aggregation of the payload, and low uptake of large objects.[18] The other active method, microinjection, is the most efficient and direct way to deliver QDs into the cytoplasm. The delivery is done via a sharp glass microcapillary tip (with a diameter <0.5 μm) that mechanically penetrates the cell membrane while maintaining reasonable cell viability.[23,24] However, the injection of large cargo (>0.5 μm) or aggregation-prone objects such as QDs and QDs−protein conjugates is difficult due to repeated tip clogging.

Here we applied the photothermal nanoblade technique[25−27] to deliver tubulin−QDs conjugates into the cytoplasm of HeLa cells. As shown in Figure 1a, a laser pulse is used to excite surface plasmons in the thin titanium coating on the tip of a glass capillary pipet; the plasmon absorption conducts heat into the liquid medium in close proximity to the metal which in turn produces nanosecond-short explosive vapor bubbles right next to the cell membrane. These bubbles produce large transient cuts or pores in the cell membrane. Concurrently, by pressurizing the capillary, a transient liquid flow is generated, enabling the delivery of the payload into the cytosol. In contrast to traditional microinjection, the photothermal nanoblade is brought in gentle contact with the cell membrane, eliminating the need for damaging, mechanical puncturing. It also allows use of a

Received: July 30, 2012
Revised: October 15, 2012
Published: October 24, 2012

   dx.doi.org/10.1021/nl302821g | *Nano Lett.* 2012, 12, 5669−5672

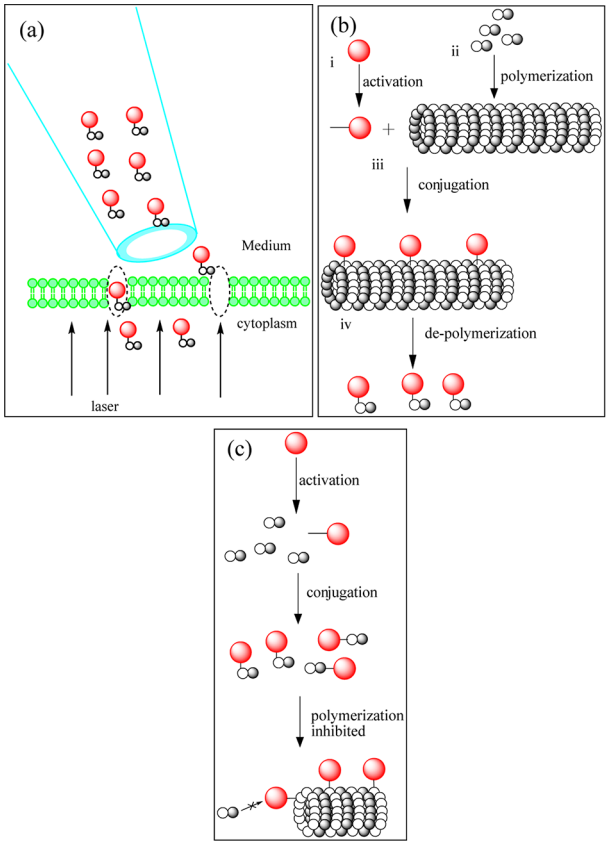

Figure 1. (a) Photothermal nanoblade delivery of tubulin−QD conjugates into the cytosol; (b) three-step tubulin−QDs conjugation strategy; (c) single-step tubulin−QD conjugation strategy.

relatively large tip orifice (up to ~2 μm) and injection of relatively large objects such as bacteria.[15]

To demonstrate successful QD delivery and cytosolic targeting, we incorporated QDs-tubulin conjugates into growing microtubules in live cells. The large size of QDs could possibly hinder the polymerization of the conjugates in growing filaments. To circumvent this, a multistep scheme was therefore devised (Figure 1b): (i) amine-derivatized, PEG-coated QDs were reacted with bis[sulfosuccinimidyl] suberate (BS3) cross-linker followed by a gel filtration step (to remove excess BS3); (ii) tubulin monomers were polymerized at 37 °C in the presence of GTP and DMSO; (iii) when the tubulin solution became turbid (due to microtubule polymerization), preactivated QDs were added to react with amine groups on polymerized tubulin molecules; and (iv) the reaction solution was quenched with hydroxylamine and centrifugation at 15 000*g* at 4 °C for 15 min. The pellet was then depolymerized at 4 °C in a DMSO-free buffer and purified by a 100K molecular weight cutoff (MWCO) centrifuge filter. As a control, a random conjugation method was also implemented (Figure 1c). The preactivated QDs were mixed with tubulin dimers, resulting in nonspecific conjugation via amine groups.

Following photothermal nanoblade delivery of depolymerized tubulin−QD conjugates (Figure 1b) to HeLa cells, filamentous structures were observed by wide-field fluorescence microscopy for long periods of times (Figure 2a,b), indicating successful delivery and targeting. Nonspecific background and incomplete filamentous structures were observed after nanoblade delivery of conjugates prepared according to the scheme described in Figure 1c, possibly due to conjugation-induced blocking of the tubulin binding site (Figure 2c). Also, nanoblade-based delivery of bare amine-derivatized PEG-coated QDs into HeLa cells resulted in interspersed punctuated spots over a uniform staining of the cytosol (Figure 2e), possibly indicating aggregation of probes in the cytosol. The above representative images (more data in the Supporting Information) showed the successful cytosol staining on microtubules. However, the effect of QDs size on cyto-staining still remains for further study. Although it has been reported that large size of QDs probes may result in multivalent conjugation, cross-linking, steric hindrance, reduced diffusion, and potential alternation of function of

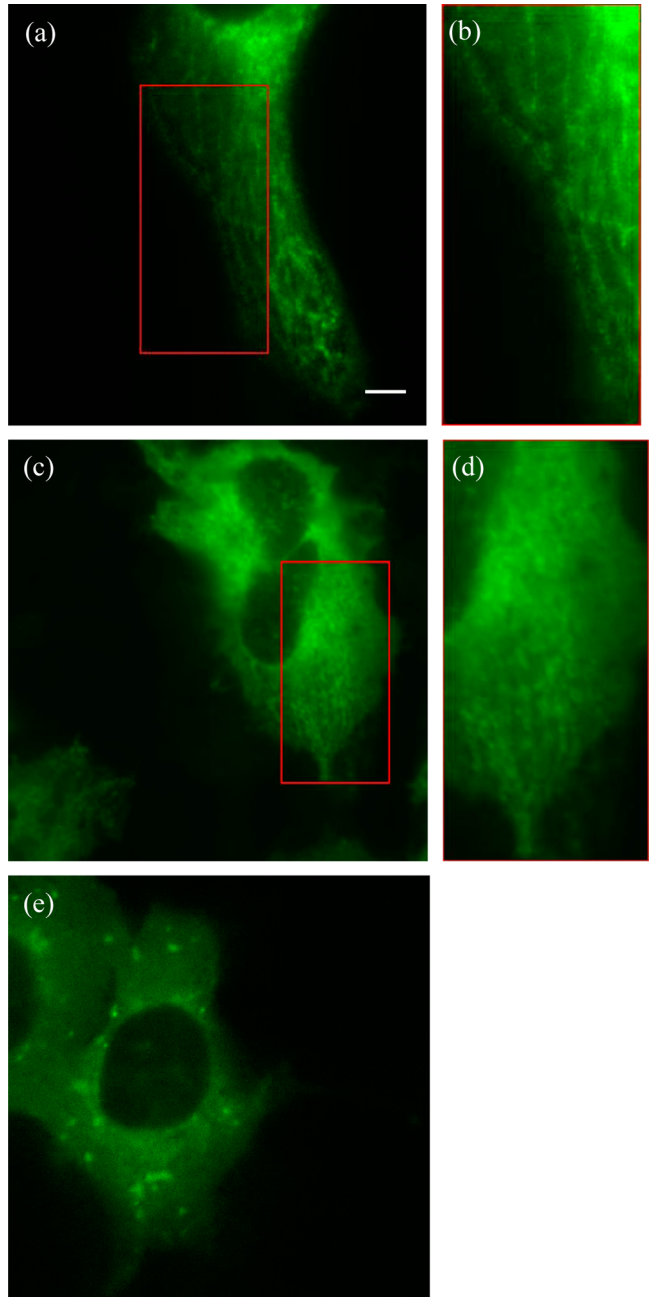

Figure 2. Images of live HeLa cells after photothermal nanoblade delivery of (a) tubulin−QD conjugates prepared with the three-step conjugation strategy (scheme in Figure 1b); (b) zoom-in of boxed area in panel a; (c) tubulin−QD conjugates prepared with the single-step conjugation strategy (Figure 1c); (d) zoom-in of boxed area in panel c; (e) bare amine-derivatized PEG-coated QDs. Scale bar: 8 μm.

dx.doi.org/10.1021/nl302821g | *Nano Lett.* 2012, 12, 5669−5672

biomolecules,[28−30] a thorough and systemic study is still needed in the future.

In order to confirm specific targeting and QD incorporation into growing filaments, cells with QD-stained filamentous structures were fixed and sequentially labeled with antitubulin IgG (mouse) followed by alexa-647 antimouse IgG (goat). Cells injected with tubulin-QDs conjugates (Figure 1b) displayed good colocalization between the QDs and the alexa-647 channels (Figures 3a−c), whereas cells injected with bare amine-derivatized

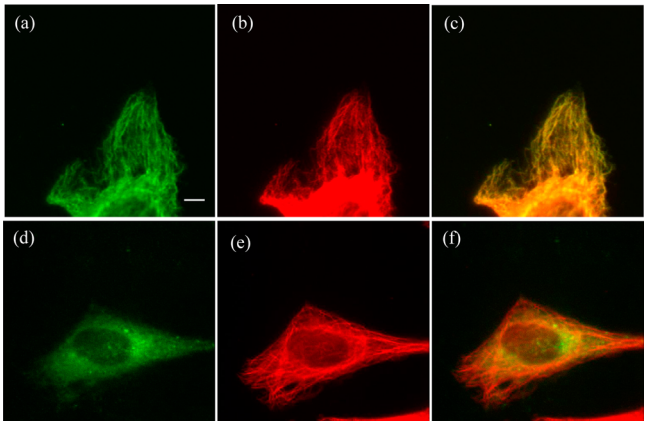

Figure 3. Images of fixed HeLa cells after photothermal nanoblade delivery of tubulin−QD conjugates (green) and immunocytochemistry labeling of tubulin (red): (a) tubulin−QD conjugates (scheme in Figure 1b); (b) immunocytochemistry image of same cell as in panel a; (c) overlay of panels a and b; (d) bare amine-derivatized PEG-coated QDs; (e) immunocytochemistry image of same cell as in panel c; (f) overlay of panels d and e. Scale bar: 8 μm.

PEG-coated QDs displayed filamentous structures only on the alexa-647 channel and poor colocalization (Figures 3d−f).

Figure 3 provides evidence for successful delivery and targeting of QDs to a cytosolic target, i.e., the polymerizing microtubule network. We also tested the delivery of the same conjugates using the conventional microinjection method. The two delivery methods were compared with regard to successful targeting and cell viability post injection (Figure 4). Cell viability was estimated by surface morphology 1 hr after injection. Conventional microinjection of amine-derivatized PEG-coated QDs was difficult (due to aggregation and clogging) but still possible. Cell viabilities post deliveries of these QDs were comparable for both methods (Figure 4). Conventional microinjection of tubulin−QDs conjugates was not at all possible for ∼0.5 μm microcapillary tips due to severe aggregation and clogging. When tip diameters were increased to ∼1 μm, some successful injections could be carried out but with greater difficulty in penetrating the cell membrane (higher mechanic force was needed to puncture the cell membrane) and with significant reduction in cell viability post injection. In contrast, photothermal nanoblade delivery was as efficient for tubulin−QDs conjugates as for amine-derivatized PEG-coated QDs, while maintaining good cell viability post injection (Figure 4). Furthermore, photothermal nanoblade delivery is significantly easier as it requires only a gentle contact on the cell membrane and therefore is devoid of failed attempts that result in broken pipet tips.

To summarize, we conjugated tubulin to QDs and successfully delivered and targeted them into growing microtubule structures inside live cells using the photothermal nanoblade delivery method. This method achieved efficient delivery of endosome-free

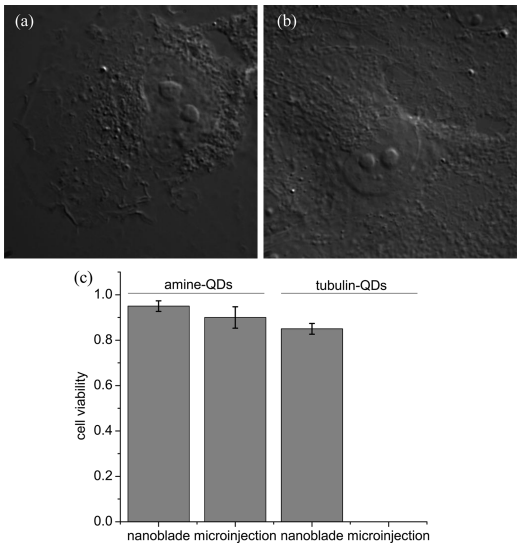

Figure 4. Examples of cell morphology after (a) microinjection and (b) photothermal nanoblade (tip ∼1 μm) delivery of tubulin−QD conjugates. (c) Cell viability postphotothemal nanoblade and conventional microinjections of bare amine-derivatized PEG-coated QDs and tubulin−QD conjugates (scheme in Figure 1b).

QD conjugates with high cell viabilities albeit at a low throughput. Nanotechnology-based solutions that are inspired by the photothermal nanoblade could potentially provide higher throughput delivery to cells in the future.

■ ASSOCIATED CONTENT

Supporting Information

Additional information about materials and methods, sample preparation, and more images. This material is available free of charge via the Internet at http://pubs.acs.org.

■ AUTHOR INFORMATION

Notes

The authors declare no competing financial interest.

■ ACKNOWLEDGMENTS

This work was supported by NIH Grant No. 5R01EB000312, NIH Grant No. 1R01GM086197, NSF (CBET 0853500 and ECCS 0901154), NIH (R21EB014456), a UC Discovery/Abraxis BioScience Biotechnology Award (#178517), and the Prostate Cancer Foundation Challenge Award. Conventional microinjection was done at the CNSI Advanced Light Microscopy/Spectroscopy Shared Facility at UCLA.

■ REFERENCES

(1) Bruchez, M.; Moronne, M.; Gin, P.; Weiss, S.; Alivisatos, A. P. *Science* **1998**, *281*, 2013.
(2) Chan, WC. W.; Nie, S. *Science* **1998**, *281*, 2016.
(3) Murray, C. B.; Kagan, C. R.; Bawendi, M. G. *Annu. Rev. Mater. Sci.* **2000**, *30*, 545−610.
(4) Alivisatos, A. P. *Nat. Biotechnol.* **2004**, *22*, 47−52.
(5) Pinaud, F.; Michalet, X.; Bentolila, L. A.; Tsay, J. M.; Doose, S.; Li, J. J.; Iyer, G.; Weiss, S. *Biomaterials* **2005**, *27*, 1679−1687.
(6) Smith, A.; Nie, S. *Nat. Biotechnol.* **2009**, *27*, 732−733.
(7) Susumu, K.; Uyeda, H. T.; Medintz, I. L.; Pons, T.; Delehanty, J. B.; Mattoussi, H. *J. Am. Chem. Soc.* **2007**, *129*, 13987−13996.
(8) Breus, W.; Heyes, C. D.; Tron, K.; Nienhaus, G. U. *ACS Nano* **2009**, *3*, 2573−2580.

(9) Michalet, X.; Pinaud, F. F.; Bentolila, L. A.; Tsay, J. M.; Doose, S.; Li, J. J.; Sundaresan, G.; Wu, A. M.; Gambhir, S. S.; Weiss, S. *Science* **2005**, *307*, 538−544.
(10) Wang, X.; Ren, X.; Kahen, K.; Hahn, M.; Rajeswaran, M.; Maccagnano-Zacher, S.; Silcox, J.; Cragg, G.; Efros, A.; Krauss, T. *Nature* **2009**, *459*, 686−689.
(11) Mahler, B.; Spinicelli, P.; Buil, S.; Quelin, X.; Hermier, J.; Dubertret, B. *Nat. Mater.* **2008**, *7*, 659−664.
(12) Chang, E.; Thekkek, N.; Yu, W.; Colvin, V.; Drezek, R. *Small* **2006**, *2*, 1412−1417.
(13) Nelson, S.; Ali, M.; Trybus, K.; Warshaw, D. *Biophys. J.* **2009**, *97*, 509−518.
(14) Ruan, G.; Agrawal, A.; Marcus, A. I.; Nie, S. *J. Am. Chem. Soc.* **2007**, *129*, 14759−14766.
(15) Medintz, I. L.; Pons, T.; Delehanty, J. B.; Susumu, K.; Brunel, F. M.; Dawson, P. E.; Mattoussi, H. *Bioconjug. Chem.* **2008**, *19*, 1785−1795.
(16) Bayles, A.; Chahal, H.; Chahal, D.; Goldbeck, C.; Cohen, B.; Helms, B. *Nano Lett.* **2010**, *10*, 4086−4092.
(17) Yezhelyev, M.; Qi, L.; O'Regan, R.; Nie, S.; Gao, X. *J. Am. Chem. Soc.* **2008**, *130*, 9006−9012.
(18) Delehanty, J. B.; Bradburne, C. E.; Boeneman, K.; Susumu, K.; Farrell, D.; Mei, B.; Blanco-Canosa, J. B.; Dawson, G.; Dawson, P. E.; Mattoussi, H.; Medintz, I. L. *Integr. Biol.* **2010**, *2*, 265−277.
(19) Buono, C; Anzinger, J.; Amar, M.; Kruth, H. *J. Clin. Invest.* **2009**, *119*, 1373−1381.
(20) Derfus, A. M.; Chan, W. C. W.; Bhatia, S. N. *Adv. Mater.* **2004**, *16*, 961−966.
(21) Chen, F. Q.; Gerion, D. *Nano Lett.* **2004**, *4*, 1827−1832.
(22) Dubertret, B.; Skourides, P.; Norris, D. J.; Noireaux, V.; Brivanlou, A. H.; Libchaber, A. *Science* **2002**, *298*, 1759−1762.
(23) Han, S.-W.; Nakamura, C.; Kotobuki, N.; Obataya, I.; Ohgushi, H.; Nagamune, T.; Miyake, J. *Nanomed. Nanotechnol. Biol. Med.* **2008**, *4*, 215−225.
(24) Zhang, Y. Nat. Protoc. http://www.natureprotocols.com/2007/11/02/microinjection_technique_and_p.php, published online November 2, 2007.
(25) Wu, T. H.; Teslaa, T.; Kalim, S.; French, C. T.; Moghadam, S.; Wall, R.; Miller, J. F.; Witte, O. N.; Teitell, M. A.; Chiou, P. Y. *Anal. Chem.* **2011**, *83*, 1321−1327.
(26) Wu, T. H.; Teslaa, T.; Teitell, M. A.; Chiou, P. Y. *Opt. Express* **2010**, *18*, 23153−23160.
(27) Wang, G.; Shimada, E.; Zhang, J.; Hong, J. S.; Smith, G.; Teitell, M. A.; Koehler, C. M. *Proc. Natl. Acad. Sci. U.S.A.* **2012**, *109*, 4840−4845.
(28) Howarth, M.; Liu, W.; Puthenveetil, S.; Zheng, Y.; Marshall, L.; Schmidt, M.; Wittrup, K.; Bawendi, M.; Ting, A. *Nat. Methods* **2008**, *5*, 397−399.
(29) Smith, A.; Wen, M.; Nie, S. *Biochem (Lond)* **2010**, *32*, 12.
(30) Jamieson, T.; Bakhshi, R.; Petrova, D.; Pocock, R.; Imani, M.; Seifalian, A. *Biomaterials* **2007**, *28*, 4717−4732.